Theoretical evaluation of adiabatic and vertical electron affinity of some radiosensitizers in solution using FEP, ab initio and DFT methods

Teodorico C. Ramalho[a], Ricardo Bicca de Alencastro[b],
Mauro Aquiles La-Scalea[c], José Daniel Figueroa-Villar[a],*

[a] *Departamento de Química, Instituto Militar de Engenharia, Praça General Tibúrcio 80, 22290-270 Rio de Janeiro-RJ, Brazil*
[b] *Grupo de Físico-Química Orgânica, Departamento de Química Orgânica, Instituto de Química, Universidade Federal do Rio de Janeiro, Ilha do Fundão, CT, Bl. A, Lab. 609, 21949-900, Rio de Janeiro-RJ, Brazil*
[c] *Departamento de Farmácia, Faculdade de Ciências Farmacêuticas, Universidade de São Paulo, Av. Lineu Prestes, 580 Bloco 13 sup. 05508-900, São Paulo-SP, Brazil*

Abstract

The biological activity of radiosensitizers is associated to their electron affinity (EA), which can be divided in two main processes: vertical and adiabatic. In this work, we calculated the EAs of nitrofurans and nitroimidazoles (Fig. 2) using Hartree–Fock (HF) and density functional theory (DFT) methods and evaluated solvent effects (water and carbon tetrachloride) on EAs. For water, we combined the polarized continuum model (PCM) and free energy perturbation (FEP) (finite difference thermodynamic integration, FDTI) methods. For carbon tetrachloride, we used the FDTI method. The values of adiabatic EA obtained are in agreement with experimental data (deviations of 0.013 eV). The vertical EAs were calculated according to Cederbaum's outer valence Green function (OVGF) method. This methodology, which relies on theoretical aspects of free energy calculations on charged molecules in solution, was used to select potential selective radiosensitizers from recently reported compounds and could be helpful in the rational design of new and more selective bioreductive anticancer drugs. © 2004 Elsevier B.V. All rights reserved.

Keywords: Radiosensitizers; Electron affinity; HF and DFT calculations

1. Introduction

It is well known that the high rate of tumor cell proliferation increases oxygen consumption in tumor tissue. Furthermore, because of poor vascularization and potentially high oxygen demand, structural and functional abnormalities in tumor vessels lead to decreased oxygen delivery to tumor tissue [1]. These hypoxic cells are resistant to radiation therapy and to some types of chemotherapy [2,3]. Therefore, tumor hypoxia can be exploited for selective anticancer drug treatment using hypoxic cell cytoxins or hypoxic cell radiosensitizers [4].

---

* Corresponding author. Tel.: +55-21-25467057; fax: +55-21-25467059.

E-mail address: figueroa@ime.eb.br (J.D. Figueroa-Villar).
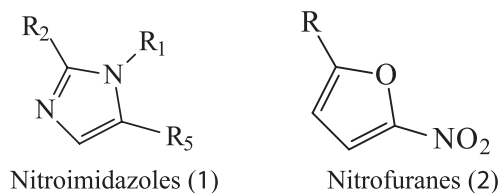
Nitroimidazoles (1)   Nitrofuranes (2)

Fig. 1. Classes of compounds used in this study.

Hypoxic cell radiosensitizers behave as oxygen-mimicking compounds, affecting tumor hypoxic cells and leading to radiation-induced damage to DNA and other molecules [5]. Thus, normally inert compounds, which are activated by enzymes or by radiation under hypoxic conditions, will behave selectively toward tumors. Ideally, the compound should be reversibly reduced so that, in normal
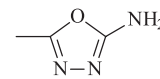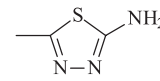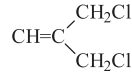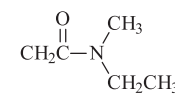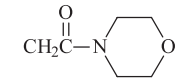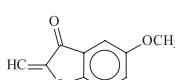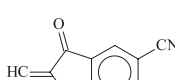
Compound	N°	R_1	R_2	R_5	Ref
5-Nitro imidazole	I.1	CH_3	H	NO_2	54
(1)	I.2	CH_2CH_2OH	H	NO_2	55
	I.3	$CH_2CH(OH)CH_3$	H	NO_2	54
	I.4	$CH_2CH_2SO_2CH_2CH_3$	H	NO_2	55
	I.5	CH_3	(oxadiazole-NH_2)	NO_2	67
	I.6	CH_3	(thiadiazole-NH_2)	NO_2	67
	I.7	$CH=C(CH_2Cl)CH_2Cl$	H	NO_2	68
2-Nitro imidazole	II.1	H	NO_2	H	54
(1)	II.2	H	NO_2	CN	69
	II.3	$CH_2C(O)-N(CH_3)CH_2CH_3$	NO_2	H	70
	II.4	$CH_2C(O)NHCH(OH)CH_3$	NO_2	H	70
	II.5	$CH_2C(O)-N$(morpholine)O	NO_2	H	70
5-Nitro furan	III.1	-	$CH=NHHCONH_2$	NO_2	71
(2)	III.2	-	CN	NO_2	71
	III.3	-	(benzofuranone-OCH_3)	NO_2	66
	III.4	-	(benzofuranone-CN)	NO_2	66

Fig. 2. Structures of all the used compounds.

cells, it could readily revert to its inactive form [6].

The biological activity of radiosensitizers is associated to their electron affinity (EA), which can be divided in two different processes: vertical and adiabatic. The first term is defined as the energy difference between the neutral molecule and its negative ion, both at their initial geometry [7,8]. The second term is defined as the energy difference between the neutral molecule and its negative ion when both are in their most stable state. This last term can also be called the electrode potential E_7^1. Before 1960, few accurate molecular EA had been determined in the gas phase, while photoelectron spectroscopy was the main experimental technique used to obtain EAs [9]. The main importance of adiabatic EA (electrode potential) is that it can be used as an auxiliary potential for the design of bioreductive anticancer drugs. Furthermore, there is abundant reliable electrode potential (E_7^1) experimental data that can be compared to theoretically obtained EAs [10–12]. On the other hand, the theoretical vertical EA can be obtained if the outer valence Green function (OVGF) method is used [13,14]. This method is state-of-the-art on ionization calculations and was utilized by Ahmed on the assignment of the photoelectron spectra of quinolines [15].

The most used radiosensitizers are nitroimidazole and nitrofuran derivatives [16,17]. Because the first nitroimidazole drugs such as dimetridazole (**I.1**) exhibit many undesired effects, there is much research in this area to be done, including studies on bioreducible groups other than nitro [18]. Lead compounds include N-oxides, quinones and transition metal complexes. However, because nitroimidazoles and nitrofurans are historically important, they are still frequently used and, there is a great deal of reliable E_7^1 data on them, thus turning them into good targets for theoretical studies. The molecules that are the subject of this study are shown in Fig. 1 [19,20]. These molecules are all structurally very similar but present significant differences between their EAs and biological activities. Also, small structural modifications confer different EA and biological activities to radiosensitizers [21], this being an interesting fact that reinforces the choice of these compounds to carry out this study. In this study, there were used representative compounds of the three most used anticancer classes of radio-

sensibilizers (2-nitroimidazoles, 5-nitroimidazoles and 5-nitrofurans, Fig. 1).

To carry out EA calculations, it is important to use good molecular hydration energy calculation methodologies. In this respect, recent calculations, which combine ab initio molecular orbital methods with free-energy perturbation methods (PMs), accomplish that goal [22,23]. In general, continuum methods for energy calculations in solution have yielded good values for the energy of hydration of molecular species [24].

The main goal of this paper are the calculation of adiabatic and vertical electron affinities of radiosensitizers (Fig. 2) using ab initio and density functional theory (DFT) methods, the evaluation of solvent effects (water and carbon tetrachloride) on EAs using the continuum model and free energy perturbation (FEP) methods, the comparison of the results with the available experimental data and, finally, the use of the methodology to select new potential radiosensitizers from compounds reported in the literature. The work is divided in two parts. In the first one, we have developed and discussed the most appropriate calculation method to obtain adiabatic EAs. In the second part, we apply the best methodology to calculate EAs of recently reported radiosensitizers candidates proposed in the literature, with the aim of selecting the most promising ones.

2. Methodology

2.1. General procedure

The calculations were carried out using the packages Spartan Pro [25], InsightII 95.0 [26] and Gaussian98w A.11 [27]. Initially, we made a conformational analysis using Monte Carlo (MC)-simulated annealing (from T=5000 K to T=300 K) [28]. Each selected conformer was fully optimized by means of two consecutive methods: semi-empirical PM3 [29] and either DFT or Hartree–Fock (HF). The difference in E_7^1 between two radiosensitizers $'Nt$ and $''Nt$ was calculated using a combination of the molecular orbital HF and DFT methods, according to the thermodynamic cycle in water and carbon tetrachloride shown in Fig. 3. The differences in free

$$'Nt(g) \; + \; ''N\bar{t}(g) \; \underset{}{\overset{\Delta G(g)}{\rightleftarrows}} \; ''Nt(g) \; + \; 'N\bar{t}(g)$$

$$\downarrow a \qquad\quad \downarrow b \qquad\qquad\quad \downarrow c \qquad\qquad \downarrow d$$

$$'Nt(aq) \; + \; ''N\bar{t}(aq) \; \underset{}{\overset{\Delta G(aq)}{\rightleftarrows}} \; ''Nt(aq) \; + \; 'N\bar{t}(aq)$$
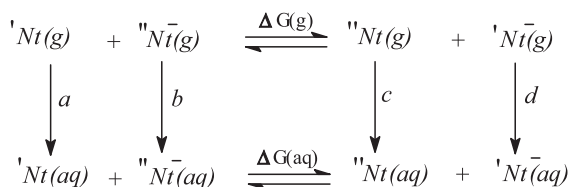
Fig. 3. Free energy perturbation cycle for the calculation of free energies of hydration.

energies of hydration between the neutral and anion pair, $(b-d)$ and $(a-c)$, were performed using FEP and PCM calculations (Eq. (1)).

$$\Delta G_{(solv)} = (d-a) + (c-b) + \Delta G_{(g)} \qquad (1)$$

The vertical EAs were calculated at the ab initio level according to Cederbaum's OVGF method [13,14], which includes the effects of electron correlation and reorganization beyond the Hartree–Fock approximation. The self-consistent part was expanded up to the third-order term.

2.2. DFT and ab initio calculations

Different levels of the DFT and ab initio (HF) methods with the basis sets 6-311++G** and 3-21+G** were used. The DFT calculations were used with the same previous basis sets. They were applied with the functional correlation of Lee, Yang and Parr, which includes both local and non-local terms [30], and Becke's 1988 functional, which includes Slater exchange along with corrections involving the gradient of electronic density [31]. After each optimization, a constant force calculation was carried out in order to verify if the optimized structures were indeed local minima (no imaginary frequencies) or transition states (one imaginary frequency) [32]. The solvent effect was evaluated with utilization of the polarized continuum model (PCM), initially proposed by Miertus and Tomasi [33] using the previous levels of theory. In this method, the solute cavity may be specified as a set of overlapping spheres, thus allowing for a more realistic cavity shape for extended molecules, in contrast to another solvation models [34]. It is interesting to note that nitroimidazoles are sensitive to the correct choice of the cavity for solvation.

2.3. FEP calculations

The bond length, bond angle, dihedral angle and non-bonded potential functions were chosen by means of the CVFF91 force field [35]. The free energy perturbation calculation of the differences in free energies of hydration between the neutral and anion pair, $(b-d)$ and $(a-c)$, was performed using the Discover 2.9.5 program (Fig. 2 and Eq. (1)) [26].

We performed successive transformation simulations, where each transformation, regardless of the environment, was achieved by an MD run of 1.2 ns using the FDTI method to compute free energy differences. The initial and final states were linearly coupled through the λ parameter. The number of quadrature points, n, used in the calculations was 6. The values of $\Delta\lambda_i$ ($\Delta\lambda 1=0.0857$, $\Delta\lambda 2=0.1804$, $\Delta\lambda 3=0.2340$, $\Delta\lambda 4=0.2340$, $\Delta\lambda 5=0.1804$, $\Delta\lambda 6=0.0857$) and the quadrature points ($\lambda 1=0.03377$, $\lambda 2=0.16940$, $\lambda 3=0.38069$, $\lambda 4=0.61931$, $\lambda 5=0.83060$, $\lambda 6=0.96623$) (see Eq. (4)) were automatically calculated by the Gaussian–Legendre quadrature method [38]. The increment $\delta\lambda$ used in Eq. (4) was 0.0005.

All transformations were performed using MD simulations in an NVT ensemble (T=300 K), employing the single topology approach. The FDTI method was employed to calculate the free energy changes in all transformations [49,50]. This method combines the formalism of the perturbation method (Eq. (2)) and of the thermodynamic integration (TI) method (Eq. (3)) to compute numerically the derivatives of the free energy in relation to the coupling parameter at fixed values of λ, followed by numerical integration using a quadrature scheme (Eq. (3)) [51]. In Eq. (3), k is the Boltzmann constant; T is the temperature; $\langle \; \rangle \lambda_i$ refers to an average over the ensemble of configurations generated using the potential energy function at λ_i ($U(\lambda_i)$); and n is the number of windows used to couple the initial and final states. In Eq. (2), the integrand is the average value of the potential energy derivative with respect to the coupling parameter λ. In Eq. (4), n is the number of quadrature points; $\Delta\lambda_i$ is a parameter that depends on the numerical integration scheme; and $\Delta\lambda$ is the increment used to compute the numerical derivatives [52].

$$\Delta A = -kT \sum_{i=1}^{n} \ln\left\langle e^{-(U(\lambda_i+\Delta\lambda)-U(\lambda_i))/kT} \right\rangle_{\lambda_i} \qquad (2)$$

$$\Delta A = \int_0^1 \left\langle \frac{\partial U(\lambda)}{\partial \lambda} \right\rangle_\lambda \mathrm{d}\lambda \tag{3}$$

$$\Delta A = -kT \sum_{i=1}^{n} \frac{\ln \left\langle \mathrm{e}^{-[U(\lambda_i + \delta\lambda) - U(\lambda_i)]/kT} \right\rangle_{\lambda_i}}{\delta\lambda} \Delta\lambda_i \tag{4}$$

In this work, the initial and final states were linearly coupled through the λ parameter. In contrast to PM, the number of λ to be used in the free energy calculations employing FDTI is not dependent on the degree of overlap of the initial and final phase spaces.

3. Results and discussion

3.1. Conformational search

The Metropolis method, also known as Monte Carlo simulated annealing, was used for the conformational search [28]. At each step in the simulation, a small random displacement was applied to each degree of freedom of the molecule and the new energy was compared with the energy of the preceding step. If the new energy was lower, the new configuration was accepted or rejected according to the value of a probability expression dependent on a defined used temperature, T. The probability of acceptance is given by:

$$P(\Delta E) = \mathrm{e}^{\frac{-\Delta E}{k_B T}} \tag{5}$$

where ΔE is the energy difference to the previous step, and k_B is the Boltzmann constant. At high enough temperatures, almost all steps are accepted. At lower temperatures, fewer high-energy structures are accepted.

The simulation proceeds as a series of cycles, each at a specified temperature. Each cycle contains a large number of individual steps, accepting or rejecting the current temperature. After a specified number of acceptances or rejections, the next cycle begins with the temperature lowered by a specified schedule such as:

$$T_i = g T_{i-1} \tag{6}$$

where T_i is the temperature at cycle i, and g is a constant between 0 and 1. Simulated annealing allows for an efficient exploration of the complex configurational space with multiple minima [28]. The initial configuration was generated randomly, considering the position and orientation of the solute molecule. One MC step is performed after randomly attempts to rotate all solute single bounds. The maximum rotation angle was fixed during the simulation as $\delta\theta=20°$. Each simulation cycle consisted of a thermalization phase of 2.0×10^6 MC steps, followed by an averaging step of 80.0×10^6 MC steps. The temperature varied from 5000 to 298 K. This procedure was chosen to perform the conformational search due to the complex landscape of minima, which flexible molecules have [36]. It was observed that in all compounds, the nitro group is in the plane of the imidazol ring (dihedral angle 1.05°). A maximum elongation of 0.010 Å occurred at the C5-NO$_2$ bond of compound **I.4**; however, this elongation was only 0.007 and 0.004 Å for compounds **I.3** and **I.2**, respectively. These results are in complete agreement with the X-ray diffraction experimental structures obtained by Walsh [37]. A relatively high rotation energy barrier for the nitro groups (14.84 kJ mol^{-1} average) was obtained from single point energy calculations using rMP2/6-311++G(d,p) for the neutral molecules and uMP2/6-311++G(d,p) for the negative ions. The bond length and the ring atom angles are in agreement with experimental data [37]. The selected conformations were subsequently refined to the ab initio and DFT levels.

The selected optimized conformations were then submitted to electrostatic charge calculations. The electrostatic charges were determined so as to reproduce the B3LYP/6-311++G** quantum molecular mechanical electrostatic potential (MEP) [38]. This means that it was necessary to produce charges that fit into the electrostatic potential at points selected according to the CHelpG scheme [39,40].

3.2. Theoretical considerations to calculate the free energy of monovalent molecules in solution

3.2.1. The FEP method

A pertinent problem when calculating solvation free energy of charged molecules and ions is how to deal with the system boundaries. In the present work,

we have chosen to employ the constrained spherical boundary model developed by Warshel and King via the Surface Constraint All-Atom Solvent (SCAAS) model [41,42]. There are considerations that make the spherical boundary more suitable than the often used Periodic Boundary Conditions (PBC). First, the use of PBC requires a rather large number of water molecules to avoid artificial distortions of the electric fields near the boundaries of the central image. It is also well known that calculated free energies are quite sensitive to the choice of cutoff radii in the simulation [43]. In the SCAAS model, the solvent is represented as an isolated sphere of water molecules surrounding the solute. It should be noted that the calculation of the free energy of charged molecules in any finite or periodic system with a finite interaction cutoff radius must include a correction to the calculated hydration energy due to the surrounding (infinite) medium. This correction can be calculated from the Born term contribution to $\Delta\Delta G_{solv}^{FEP}$ [43,44]. In order to minimize the dependency of the calculated $\Delta\Delta G_{solv}^{FEP}$ with the system size, the computation time and the Born term contribution, we decided to obtain the aqueous phase by surrounding the studied molecules with a water sphere of 15 Å centered at the N1 atom of each compound, including a total of about 350 water molecules. It was also employed the spherical boundary model (SCAAS) assuming the Born radius (radius of the cavity in the macroscopic medium) equal to the sphere radii of all the studied compounds ($R_{SCAAS} = r_{Born} = 15$ Å) [41,42].

3.2.2. The PCM method

The original version of PCM defines the cavity as an envelope of spheres centered on atoms (or at the most atomic groups) [33]. Due to the fact that the cavity definition in continuum solvation methods is a well-known aspect which has led to many different studies of systematic nature [45], we, in the present study, define the cavity in terms of spheres centered on atoms and with radii, $\Re_\varsigma$, proportional to van der Waals radii (see Eq. (7)).

$$\Re_\varsigma = f\Re_\varsigma^{vdW} \qquad (7)$$

Chosen as scaling factors (f) for the calculations for neutral solutes in water and carbon tetrachloride were 1.25 and 1.80, respectively [46,47]. Moreover,

for charged compounds, we found it necessary to reduce the atomic radii of the atom(s) bearing the charge by about 10% [48].

3.3. Validation of the theoretical model for EA calculations in aqueous solutions

All discussions concerning the energy differences and the energy barriers refer to the enthalpy term, corrected for the zero point energy (ZPE) at 298.15 K. The relative adiabatic EAs were calculated according to the thermodynamic cycle shown in Fig. 2. All calculations were relative to 2-nitroimidazole ($E_7^1 = -0.418$ eV). This process was carried out in two steps. First, the most appropriate quantum method for the calculation of the gas phase contribution, $\Delta G(g)$, was chosen, while $\Delta G(aq)$ was calculated using FEP-CVFF91 (step A). Then, in the second step, the most appropriate method to calculate the free energy of hydration was chosen, while the gas phase contribution was kept constant. The compounds used for this validation procedure were chosen from representative families of radiosensitizers (I.1–4, II.1 and III.1, Fig. 2).

The relaxation energy of the negative ion was obtained using the optimized geometries at the HF and DFT levels. The solvent effect, ($b-d$) and ($a-c$) (see Fig. 2), was evaluated with the polarized continuum model [33] and FEP with the finite difference thermodynamic integration (FDTI) method [49]. The results for the two methodologies are similar (see Table 1), but the values obtained for the relative hydration free energy from FEP calculations with B3LYP/6-311++G** allow for a better calculation of adiabatic EA as compared with the experimental data.

In step A, it was used FEP-CVFF91 to calculate free energy of hydration at several levels of calculation to obtain the gas phase free energy. There were observed large differences (about 0.126 eV) between the results obtained with the HF/3-21+G** and HF/6-311++G** basis set. The values obtained using B3LYP/3-21+G** and B3LYP/6-311++G** are closer, with a difference of only about 0.054 eV. Thus, the last values, obtained using DFT calculations, demonstrated better accuracy when compared to the experimental data than the values obtained using HF calculations (Table 1).

Table 1
Adiabatic electron affinities (in electronvolts) calculated with a combination of FEP-CVFF91/gas phase Quantum Mechanic calculations and PCM/B3LYP/6-311G** gas phase Quantum Mechanic calculations

	I.1	**I.2**	**I.3**	**I.4**	**II.1**	**II.2**	**III.1**
Step A							
HF/3-21+G**	−0.639	−0.736	−0.669	−0.713	−0.664	−0.514	−0.504
HF/6-311++G**	−0.509	−0.616	−0.541	−0.587	−0.539	−0.390	−0.376
B3LYP/3-21+G**	−0.460	−0.552	−0.501	−0.527	−0.489	−0.339	−0.327
B3LYP/6-311++G**	−0.400	−0.501	−0.444	−0.477	−0.431	−0.282	−0.270
Step B							
HF/3-21+G**	−0.708	−0.810	−0.713	−0.776	−0.700	−0.547	−0.553
HF/6-311++G**	−0.570	−0.668	−0.576	−0.609	−0.600	−0.448	−0.440
B3LYP/3-21+G**	−0.526	−0.624	−0.570	−0.603	−0.556	−0.404	−0.396
B3LYP/6-311++G**	−0.463	−0.563	−0.507	−0.539	−0.493	−0.344	−0.333
Experimental							
	−0.388[a]	−0.486[b]	−0.431[a]	−0.464[b]	−0.418[c]	−0.267[d]	−0.257[e]

A: Combination of FEP-CVFF91 and gas phase Quantum Mechanic calculations. B: Combination of PCM and gas phase B3LYP/6-311++G** Quantum Mechanic calculations.

[a] Ref. [54].
[b] Ref. [55].
[c] Ref. [69].
[d] Ref. [1].
[e] Ref. [70].

The estimated error in the calculation of adiabatic electron affinity in step A was 0.013 eV (RMS=0.001 eV) using B3LYP/6-311++G**, 0.068 eV (RMS=0.004 eV) with B3LYP/3-21+G**, 0.121 eV (RMS=0.007 eV) using HF/6-311++G** and 0.247 eV (RMS=0.006 eV) when HF/3-21+G** was combined with FEP.

Other functions of non-local densities, such as B-VWN, gave random errors and the wave-function-based approaches gave systematic errors [53].

The adiabatic EA values for all the nitro compounds are shown in Table 1. It can be observed, in step A, that the calculation at the DFT level with the basis set 6-311++G** is in better agreement with the experimental data [54,55]. When B3LYP/6-311++G** was combined with the FEP calculation we found EA value deviations only in the range of 0.013 eV, as compared with experimental data [54,55]. This method is interesting, as it includes the effect of electronic correlation, and allows for the calculation of bigger systems. Thus, B3LYP/6-311++G** was selected as the most appropriate quantum method for calculations of the gas phase free energy. This conclusion is in agreement with calculations carried out by Guo-xin, which showed

the greater efficiency of DFT calculations for charged molecules [56].

In step B, PCM was used at several levels of calculation to obtain the free energy of hydration. PCM was also used at the DFT level (B3LYP) with the basis set 6-311++G ** to calculate the gas phase free energy. It was observed also a large difference (about 0.140 eV) between the results obtained with HF/3-21+G** and HF/6-311++G**. The values obtained using DFT (B3LYP/3-21+G** and B3LYP/6-311++G**) are closer, with a difference of only about 0.063 eV. It could be concluded that DFT calculations demonstrated better accuracy when compared to the experimental data than the values obtained using HF calculations (Table 1).

The adiabatic EA calculated values for all the nitro compounds are shown in Table 1. It can be also observed, in step B, that the calculation at the DFT level with the basis set 6-311++G** is in better agreement with the experimental data [54,55]. When B3LYP/6-311++G** was combined with the PCM-B3LYP/6-311++G** calculation we found EA value deviations in the range of 0.088 eV as compared with experimental data [54,55].

The estimated error in the calculation of adiabatic electron affinity was of 0.088 eV (RMS=0.001 eV) using PCM-B3LYP/6-311++G**, 0.138 eV (RMS= 0.005 eV) with PCM-B3LYP/3−21+G**, 0.170 eV (RMS=0.017 eV) with HF/6-311++G** and 0.309 eV (RMS=0.019 eV) using PCM-HF/3-21+G**.

We noticed that to estimate the free energy of hydration the FEP method is slightly superior to the polarized continuum model. This is particularly true when intermolecular hydrogen bonding occurs in ionic solutions. Similar results are found in the literature [57,58].

The most important result is that the adiabatic electron affinity can be calculated with average errors of 0.013 eV, using FEP-CVFF91 combined with B3LYP/6-311++G**, and 0.088 eV, using PCM-B3LYP/6-311G** combined with B3LYP/6-311++G**. A priori, we believe that these small deviations could be due to different reasons, such as intrinsic shortcomings of the PCM algorithm and inaccuracy of the non-polarizable force field parameters for the nitro compounds. Recent experimental and theoretical investigations on the electrode potential of 1,4-diaminobenzene lead to average errors of 0.026 eV [57,58].

It was observed that the utilization of the HF method underestimates the adiabatic EA values, while the values from DFT methods are in better agreement with the experimental data [54,55]. One reason for this may be that the correlation potential considered in our DFT approach, which is better than in the HF calculations, is very important. Another important advantage of DFT is that it can easily provide an explanation for the binding of an extra electron in an anion [59].

The experimental error is, in average, ± 0.010 eV [54,55]. The smallest estimated errors in the calculation of adiabatic electron affinities were 0.013 eV (RMS=0.001 eV) when B3LYP/6-311++G** was combined with the FEP and 0.088 eV (RMS=0.001 eV) when PCM-B3LYP/6-311++G** was combined also with B3LYP/6-311++G**. These results show that the two theoretical approaches are different. Other authors have obtained similar conclusions when applying the methods to other systems [57,58].

The average EA experimental error from the literature was of ± 0.010 eV [54,55]. The average error bars in FEP calculations were ± 0.012 and ± 0.007 eV

for the ionic and neutral forms, respectively, indicating a very good precision in the calculation of the Gibbs free energy of hydration. It should be stressed that the difficulties in measuring adiabatic electron affinities in water for such reactive molecules reinforce the importance of a theoretical approach to this problem.

3.4. Adiabatic electron affinity calculation in carbon tetrachloride solution

In order to check the influence of the solvent nature on the stability of the reaction intermediates, and to obtain data that could allow for a proposal for the mechanism of biological action of these drugs, we carried out adiabatic electron affinity calculations evaluating solvent-dependent EAs in carbon tetrachloride [1,5,40]. This solvent can be used as a pharmacokinetic model to estimate relative permeability in membranes, with a water/CCl_4 biphasic system as a mimic for the water–membrane system [60]. According to the results shown in the former section, the values obtained for adiabatic EAs from FEP calculations with B3LYP/6-311++G** are in a better agreement with the experimental data [54,55]. Probably, this is due to the way that electronic charges are evaluated in the PCM method. As already noted by Tomasi et al. [61], the evaluation of electronic charges could be a delicate point in PCM because the presence of fractions of the solute charge outside the cavity can affect the result in a quite sensitive way. In recent years, the integral equation formalism (IEF) method was introduced to solve the electrostatic solvation problem at the quantum mechanical level with aid of apparent surface charges (ASC) [62]. IEF uses a new formalism for this problem, which is based on integral operators, and it manages to deal with the same footing linear isotropic solvent models, as well as anisotropic liquid crystals and ionic solutions [61]. Recently, this formalism was implemented in the PCM method [63]. Accordingly, the adiabatic EAs were obtained from the thermodynamic cycle (Fig. 2) and Eq. (1)—where the differences in free energies of solvation between the neutral and anionic pair, $(b-d)$ and $(a-c)$, were calculated using FEP with the integration method FDTI. The Born term contribution to $\Delta \Delta G_{\text{solv}}^{\text{FEP}}$ was included in the method, as well as the constrained spherical boundary model (SCAAS) [41–

44]. The studied molecules were surrounded by a carbon tetrachloride solvation sphere of 15 Å, centered at the N1 atom of each compound. All calculations were relative to 2-nitroimidazole. The results are shown in Table 2 and show that there is a decrease on the adiabatic EA in this solvent. This is probably due to a lower stabilization of the ionized form in carbon tetrachloride. Using Eq. (8), we can determine the relative equilibrium constant of the reduction reaction of all the studied compounds (Figs. 1 and 2) in water and carbon tetrachloride.

$$\ln\left(\frac{K_{H_2O}}{K_{CCl_4}}\right)$$
$$= \frac{\Delta G_{CCl_4} - \Delta G_{H_2O}}{RT} \Leftrightarrow \frac{\Delta\Delta G_{solv}(CCl_4 \to H_2O)}{RT} \quad (8)$$

In accordance with Table 2, the nitrocompounds reduction reaction is more favorable in water than in carbon tetrachloride. This conclusion supports the proposition, regarding the biological action mechanism of these compounds, that the reduction probably

Table 2
Gibbs free energy (in electronvolts) of the reduction reactions in water and carbon tetrachloride using FEP-CVFF91/B3LYP/6-311++G**

Compound	ΔG_{H_2O} (eV)	ΔG_{CCl_4} (eV)	$\ln(K_{H_2O}/K_{CCl_4})$
I.1	−0.388[a]	+0.641	40.05
I.2	−0.486[b]	+1.086	61.19
I.3	−0.431[a]	+0.964	54.29
I.4	−0.464[b]	+0.638	42.89
I.5	−0.495	+1.066	61.74
I.6	−0.502	+1.041	61.03
I.7	−0.512	+1.105	63.96
II.1	−0.418[c]	+0.941	53.75
II.2	−0.267[d]	+0.615	34.88
II.3	+0.998	+0.595	15.93
II.4	+1.130	+0.581	21.71
II.5	+1.040	+0.569	18.63
III.1	−0.257[e]	+0.611	34.33
III.2	−0.343	+0.635	38.68
III.3	−0.281	+0.623	35.75
III.4	−0.301	+0.612	36.11

[a] Ref. [54].
[b] Ref. [55].
[c] Ref. [69].
[d] Ref. [1].
[e] Ref. [70].

does not occur in the membrane, but inside the cell at the cytoplasm or at the cytoplasm–membrane interfaces [1,5,40].

3.5. Vertical electron affinity calculation

In this work, the vertical EA was calculated in the gas phase using an approach based on electronic propagator methods. Propagator methods are ideal for the study of PES [14]. A semi-direct version of the OVGF approximation was reported in the Gaussian98 A.11 only at the Hartree–Fock level. This method is a powerful tool for the computation of outer valence electron affinities, and is based on the addition of a self-energy term, $\Sigma(\hat{w})$, to the Fock operator, $\hat{F}$, in the Hartree–Fock theory (see Eqs. (9) and (10)):

$$[\hat{F} + \Sigma(\hat{w})]\Psi_i = w_i\Psi i \quad (9)$$

For a molecule with N electrons, these terms are exactly the negative of the terms for the electron removal energies:

$$w_I = E_0^{(N)} - E_I^{(N-1)} \quad (10)$$

The eigenfunctions enter into the calculation of the ionization spectral intensities [13,14]. Table 3 shows that the vertical electron affinities, when calculated at the HF/6-311++G** level, increase from **I.1** to **I.4** for 5-nitroimidazoles, from **II.2** to **II.4** for 2-nitroimidazoles and from **III.2** to **III.4** for 5-nitrofurans. This is probably due to the lower electronegativity of the substituent at position 2 of the imidazole ring. Therefore, the vertical EAs follow the tendency of the adiabatic EAs. The energy cost for the molecular reorganization (cost=|vertical EA−adiabatic EA|) increases from 0.081 eV in compound **II.5** to 1.485 eV in compound **I.4**, as compared with experimental adiabatic EA data (Table 3).

The energy cost for molecular reorganization in carbon tetrachloride is lower than in water, and it increases from 0.021 eV in compound **I.1** to 0.436 eV in compound **II.4** (Table 3). It was observed that carbon tetrachloride induces much smaller changes on the structural parameters of all the studied compounds than the changes found in water. For both

Table 3

Energy cost for the molecular reorganization difference in water (experimental data) and carbon tetrachloride (calculated using PCM-B3LYP/6-311++G**)

Compound	Vertical EA HF/6-311++G** (eV)	ΔE_{H_2O} (eV)	ΔE_{CCl_4} (eV)
I.1	0.620	1.008	0.021
I.2	0.658	1.144	0.428
I.3	0.905	1.336	0.059
I.4	1.021	1.485	0.383
I.5	0.806	1.301	0.260
I.6	0.810	1.312	0.231
I.7	0.902	1.414	0.203
II.1	0.678	1.096	0.263
II.2	0.650	0.917	0.035
II.3	0.745	0.253	0.150
II.4	1.017	0.113	0.436
II.5	0.959	0.081	0.039
III.1	0.687	0.944	0.076
III.2	0.654	0.997	0.019
III.3	0.712	0.993	0.089
III.4	0.721	1.022	0.109

solvents, it was also observed that the energy cost is proportional to the conformational flexibility.

3.6. Substituent effect

It is well known that the EA of a radiosensitizer is responsible for 80% of its biological action [66,67]. In addition, EA values show better correlation with biological activities of radiosensitizers than LUMO energies [68,71]. Thus, in this step, we performed EA calculations on a series of new radiosensitizers from the literature. This was done with the aim to estimate their comparative biological activity based on EA calculations and to identify potential pharmacophoric groups. For the EA calculations, we chose the method employed in step A, which affords a better accuracy. Our results confirm what is well known from literature, [64,65] that is, the dipole moment increases as the adiabatic EA decreases (Table 4). It is known that radiosensitizer candidate compounds should have EAs smaller than oxygen [5]. On the other hand, compounds that present EA values which are too negative have their redox properties significantly affected by the presence of small amounts of oxygen, this resulting in a redox system known as futile cycle [1], thus leading to a loss of the selectivity [1,5]. This

explains the fact that nitrofurans are easily reduced in both aerobic and anaerobic cells.

Actually, the fact that compounds **I.1** and **II.2** are structurally similar but have different EAs shows the importance of a theoretical approach to calculate with accuracy electronic properties in solution. We feel that we can confirm our methodology as appropriate for reproducing experimental EA values with the aim of proposing novel anticancer drugs. For example, experimental studies indicate that the biological action of radiosensitizers is inversely proportional to their adiabatic EA [10]. Then, according to our calculations, the selectivity towards hypoxic cells of the nitrofuran derivatives could be improved by introducing electron-withdrawing groups at position 2 of the furan ring, as this modification would lead to decreased adiabatic and vertical electron affinities. The same could be the case for the introduction of electron-withdrawing groups at C2 of 5-nitroimidazol derivatives and at C1 of 2-nitroimidazol derivatives. Accordingly, we have elected compounds **I.7** and **III.2** as potential more selective radiosensitizer candidates.

Table 4

Values of adiabatic EAs and dipole moments for all the used compounds obtained from B3LYP/6-311G** calculations

Compound	ΔG_{H_2O} (eV)	Dipole (Debye)
I.1	−0.388[a]	4.219
I.2	−0.486[b]	4.642
I.3	−0.431[a]	5.118
I.4	−0.464[b]	5.209
I.5	−0.495	5.304
I.6	−0.502	5.415
I.7	−0.512	5.502
II.1	−0.418[c]	4.315
II.2	−0.267[d]	4.003
II.3	+0.998	2.523
II.4	+1.130	2.465
II.5	+1.040	2.514
III.1	−0.257[e]	4.016
III.2	−0.343	4.186
III.3	−0.281	4.034
III.4	−0.301	4.045

[a] Ref. [54].
[b] Ref. [55].
[c] Ref. [69].
[d] Ref. [1].
[e] Ref. [70].

4. Concluding remarks

The solvation properties of electrolytes in solution are of particular importance in chemistry. This is especially so in many chemical and biochemical processes, where ionic hydration plays a very important role. In this work, we have shown an efficient theoretical approach for the calculation of the adiabatic electron affinity of a series of radiosensitizers in solution relative to 2-nitroimidazole using OVGF methods. We have shown that gas phase electronic structure calculations using B3LYP/6-311++G**, in combination with free energy of hydration (force field CVFF91) calculations, is a powerful tool for calculating one-electron adiabatic electron affinities for nitromidazole and nitrofuran derivatives in water. We also found that the free-energy perturbation method, implemented within a molecular dynamics framework using the FDTI method, was better than the PCM method for determining the free energies of hydration when intermolecular hydrogen bonding occurs. The values of the EAs obtained in this way are in agreement with experimental data (deviations of 0.013 eV). Also, the values of vertical EA, obtained with HF/6-311++G**, were used to calculate the energy cost of molecular reorganization.

We believe that the care with the several theoretical aspects in this work is responsible for the small deviation (0.013 eV) obtained in the adiabatic EA in comparison with experimental data, for example, (1) the use of Metropolis to explore the conformational space of the molecules in the gas phase; (2) the use of the DFT method to calculate the free energy contribution in the gas phase (B3LYP/6-311++G**); (3) the use of adequate scaling factors for PCM calculations (reduction of 10% in the atomic radii of the atom(s) in the charged molecules); (4) carrying out the FEP calculations with the FDTI method; (5) the use of the Born term contribution to $\Delta\Delta G_{solv}^{FEP}$, (6) the use of the constrained spherical boundary model (SCAAS). It is also likely that the magnitude of the discrepancy between calculated and experimental data is due, in part, to experimental difficulties in measuring adiabatic electron affinities in water for such reactive molecules; thus, reinforcing the importance of a theoretical approach to this problem. Our calculations also support one experimentally based proposition: that the reduction reactions do not occur in the membrane but inside the cell or at the cytoplasm–membrane interfaces.

We strongly feel that this study could be helpful for the design and selection of new and more selective bioreductive anticancer drugs. Accordingly, we were able to use our methodology to select, from several literature possibilities, two compounds, **I.7** and **III.2**, as radiosensitizers which should be potentially more selective than the ones used conventionally.

References

[1] S. Kasai, H. Nagasawa, M. Yamashita, New antimetastatic hypoxic cell radiosensitizers: design, synthesis, and biological activities of 2-nitroimidazole-acetamide, TX-1877, and its analogues, Bioorg. Med. Chem. 9 (2001) 453–464.

[2] B.A. Teicher, Hypoxia and drug-resistance, Cancer Metastasis Rev. 13 (1994) 139–168.

[3] A. Tomida, T. Tsuruo, Drug resistance mediated by cellular stress response to the microenvironment of solid tumors, Anti-Cancer Drug Des. 14 (1999) 169–175.

[4] J.M. Brown, B.G. Wouters, Apoptosis p53 and tumor cell sensitivity to anticancer agents, Cancer Res. 59 (1999) 1391–1399.

[5] H. Horis, H. Nagasawa, H. Terada, Advances in Environmental Science and Technology: Oxidants in the Environment, Wiley, New York, 1994.

[6] C. Viodé, N. Bettache, Enzymatic reduction studies of nitro-heterocycles, Biochem. Pharmacol. 57 (1999) 549–557.

[7] M. Chen, D. Moir, F.M. Benoit, et al., Purification and identification of several sulphonated azo dyes using reversed-phase preparative high-performance liquid chromatography, J. Chromatogr., A 825 (1998) 37–44.

[8] Y. Bu, Y. Liu, C. Deng, Correlation study of Franck–Condon barriers associated with electron self-exchange reactions with ionization potentials and electron affinities and experimental Born–Oppenheimer potentials, J. Mol. Struct., THEOCHEM 422 (1998) 219–228.

[9] A. Pramann, K. Rademann, Photoelectron spectroscopy of ReO^{2-} and ReO^{3-}, Chem. Phys. Lett. 343 (2001) 99–104.

[10] M.A. La-Scalea, S.H.P. Serrano, I.G.R. Gutz, Voltammetric behaviour of metronidazole at mercury of metronidazole at mercury electrodes, J. Braz. Chem. Soc. 10 (1999) 127–135.

[11] A.M.O. Brett, S.H.P. Serrano, I. Gutz, M.A. La-Scalea, M.L. Cruz, Voltammetric behavior of nitroimidazoles at a DNA-biosensor, Electronal 9 (1997) 1132–1137.

[12] M.A. La-Scalea, A.M.O. Brett, S.H.P. Serrano, DNA-modified electrodes: a new alternative for electroanalysis, Quím. Nova 22 (1999) 417–424.

[13] J.V. Ortiz, Electron-binding energies of anionic alkali–metal atoms from partial 4th-order electron propagator theory calcultions, J. Chem. Phys. 89 (1988) 6348–6352.

[14] W. von Niessen, J. Schirmer, L.S. Cederbaum, Computational

methods for the one-particle Green-function, Comput. Phys. Rep. 1 (1984) 57–125.

[15] A.A. Ahmed, M. Julliard, F. Chanon, M. Chanon, F. Gracian, G. Pfister-Guillouzo, Photoelectron spectroscopy of quinoline derivatives. Correlation of experimental ionization potentials with calculated molecular energies, Spectrochim. Acta, Part A: Mol. Biomol. Spectrosc. 53 (1997) 335–343.

[16] H. Hori, C.Z. Jin, M. Kiyono, S. Kasai, M. Shimamura, S. Inayama, Design, synthesis, and biological activity of anti-angiogenic hypoxic cell radiosensitizer haloacetylcarbamoyl-2-nitroimidazoles, Bioorg. Med. Chem. 5 (1997) 591–599.

[17] J.D. Chapamn, L.R. Coia, C.C. Stobe, E.L. Engelhart, M.C. Fenning, R.F. Schneider, Prediction of tumour hypoxia and radioresistance with nuclear medicine markers, Br. J. Cancer 74 (1996) S204–S208.

[18] J.R. Ames, M.D. Ryan, P. Kovaic, Mode of action of antiprotozoan agents—electron-transfer and oxy radicals, Life Sci. 41 (1987) 1895–1902.

[19] B. Halliwell, J.M.C. Gutterridge, Free Radicals in Bilogy and Medicine, Oxford Univ. Press, New York, 1985.

[20] A.M.O. Brett, S.H.P. Serrano, M.A. La-Scalea, Mechanism of interaction of in situ produced nitroimidazole reduction derivatives with DNA using electrochemical DNA biosensor, Methods Enzymol. 300 (1999) 314–321.

[21] G.E. Adams, I.R. Flockhart, C.E. Smithen, I.J. Straford, P. Wardman, M.E. Watts, Effects of structure and hyperthermia on radiosensitizing and differential citotoxic properties of hypoxic cell sensitizers, Radiat. Res. 67 (1976) 550–551.

[22] C.A. Reynolds, P.M. King, W.G. Richards, Accurate redox potentials from theoretical calculations—methyl-substituted benzoquinones, J. Chem. Soc., Chem. Commun. 21 (1988) 1434–1436.

[23] S.G. Lister, C.A. Reynolds, W.G. Richards, Energetics of reactions involving radical species in solution: calculation of relative electrode potentials for nitroimidazoles using density functional and continuum methods, Int. J. Quant. Chem. 59 (1997) 135–145.

[24] R. Jarger, S.M. Kast, Quantification and visualization of molecular-surface flexibility, J. Mol. Graph. Model. 13 (2001) 89–97.

[25] PC Spartan Pro 1.0.1, Wavefunction, 18401 Von Karman Avenue, Suite 370, Irvine, CA 92612 USA.

[26] Biosym/MSI, Insight II, version 95.0, Biosym/MSI, San Diego, 1995.

[27] M.J. Frisch, G.W. Trucks, H.B. Schlegel, G.E. Scuseria, M.A. Robb, J.R. Cheeseman, V.G. Zakrzewski, J.A. Montgomery, Jr., R.E. Stratmann, J.C. Burant, S. Dapprich, J.M. Millam, A.D. Daniels, K.N. Kudin, M.C. Strain, O. Farkas, J. Tomasi, V. Barone, M. Cossi, R. Cammi, B. Mennucci, C. Pomelli, C. Adamo, S. Clifford, J. Ochterski, G.A. Petersson, P.Y. Ayala, Q. Cui, K. Morokuma, P. Salvador, J.J. Dannenberg, D.K. Malick, A.D. Rabuck, K. Raghavachari, J.B. Foresman, J. Cioslowski, J.V. Ortiz, A.G. Baboul, B.B. Stefanov, G. Liu, A. Liashenko, P. Piskorz, I. Komaromi, R. Gomperts, R.L. Martin, D.J. Fox, T. Keith, M.A. Al-Laham, C.Y. Peng, A. Nanayakkara, M. Challacombe, P.M.W. Gill, B. Johnson, W. Chen, M.W. Wong, J.L. Andres, C. Gonzalez, M. Head-Gordon, E.S. Replogle, and J.A. Pople, Gaussian, Pittsburgh PA, 2001.

[28] P. Hohenberg, W. Kohn, Inhomogeneous electron gas, Phys. Rev., B 136 (1964) B864–B869.

[29] J.J.P. Stewart, Optimization of parameters for semiempirical methods, J. Comput. Chem. 10 (1989) 209–220.

[30] A.D. Becke, Density-functional exchange energy approximation with correct asymptotic-behavior, Phys. Rev., A 38 (1988) 3098–3100.

[31] W. Kohn, L.J. Sham, Self-consistent equations including exchange and correlation effects, Phys. Rev. 140 (1965) A1133–A1140.

[32] D.J. Motta-Neto, M.C. Zerner, R. Bicca de Alencastro, On the implications of the structure of 3′-azido-3′ deoxythymidine and related-compounds to antiviral activity, Int. J. Quantum Chem., Quantum Chem. Symp. 44 (1992) 743–757.

[33] S. Miertus, E. Scrocco, J. Tomasi, Electrostatic interaction of a solute with a continuum—a direct utilization of ab initio molecular potentials for the prevision of solvent effects, Chem. Phys. 55 (1981) 117–129.

[34] C. Colominas, F.J. Luque, J. Teixido, Cavitation contribution to the free energy of solvation. Comparison of different formalisms in the context of MST calculations, Chem. Phys. 240 (1999) 253–264.

[35] P. Dauber-Osgutorpe, V.A. Roberts, D.G. Osgutorpe, Structure and energetics of ligand-binding to proteins—*Escherichia coli* dihydrofolate reductase trimethoprim, a drug–receptor system, Proteins 4 (1988) 31–47.

[36] C. Colominas, F.J. Luque, M. Orzco, Monte Carlo MST: new strategy for representation of solvent configurational space in solution, J. Comput. Chem. 20 (1999) 665–678.

[37] A.J. Bracuti, Crystal structure of 4,5-dinitroimidazole (45DNI), J. Chem. Crystallogr. 28 (1998) 367–371.

[38] C.M. Breneman, K.B. Wiberg, Determining atom-centered monopoles from molecular electrostatic potentials—the need for high sampling density in formamide conformational-analysis, J. Comput. Chem. 11 (1990) 361–373.

[39] U.C. Singh, P.A. Kollman, An approach to computing electrostatic charges for molecules, J. Comput. Chem. 5 (1984) 129–145.

[40] P. Goldman, R.L. Koch, T.C. Yeung, Comparing the reduction of nitroimidazoles in bacteria and mammalian-tissues and relating it biological-activity, Biochem. Pharmacol. 35 (1986) 43–51.

[41] A. Warshel, G. King, Polarization constraints in molecular-dynamics simulation of aqueous-solutions—the surface constraint all atom solvent (SCAAS) model, Chem. Phys. Lett. 121 (1985) 124–129.

[42] G. King, A. Warshel, A surface constrained all-atom solvent model for effective simulations of polar solutions, J. Chem. Phys. 91 (1989) 3647–3661.

[43] T.P. Straatsma, H.J.C. Berendsen, Free-energy of ionic hydration-analysis of a thermodynamic integration technique to evaluate free-energy differences by molecular dynamics simulations, J. Chem. Phys. 89 (1988) 5876–5886.

[44] J. Aqvist, Ion water interaction potentials derives form free-

energy perturbation simulations, J. Phys. Chem. 94 (1990) 8021–8024.

[45] J. Tomasi, M. Perisco, Molecular-interactions in solution—an overview of methods based on continuous distributions of the solvent, Chem. Rev. 94 (1994) 2027–2094.

[46] M. Bachs, M. Orzco, F.J. Luque, Optimization of solute cavities an van-der-Waals parameters in ab-initio MST–SCRF calculations of neutral molecules, J. Comput. Chem. 15 (1994) 446–454.

[47] M. Bachs, M. Orzco, F.J. Luque, Extension of MST/SCRF method to organic solvents: ab initio and semiempirical parameterization for neutral solutes in CCl_4, J. Comput. Chem. 17 (1996) 806–820.

[48] M. Orozco, F.J. Luque, Optimization of the cavity size for ab-initio MST–SCRF calculations of monovalent ions, Chem. Phys. 182 (1994) 237–248.

[49] M. Mezei, The finite-difference thermodynamic integration, tested on calculating the hydration free-energy difference between acetone and dimethylamine in water, J. Chem. Phys. 86 (1987) 7084–7088.

[50] C.R.W. Guimarães, R. Bicca de Alencastro, Thermodynamic analysis of thrombin inhibition by benzamidine and *p*-methylbenzamidine via free-energy perturbations: inspection of intraperturbed-group contributions using the finite difference thermodynamic integration (FDTI) algorithm, J. Phys. Chem., B 106 (2002) 466–476.

[51] P. Kollman, Free-energy calculations—application to chemical and biochemical phenomena, Chem. Rev. 93 (1993) 2395–2417.

[52] W.H. Press, B.P. Flanney, S.A. Teukolsky, W.T. Vetterling, Numerical Recipes. The Art of Scientific Computing, Cambridge Univ. Press, CV Cambridge, UK, 1986.

[53] B.G. Johnson, P.M. Gill, J.A. Pople, The performance of a family of density functional methods, J. Chem. Phys. 98 (1993) 5612–5626.

[54] P. Wardman, E.D. Clarke, One-electron reduction potentials of substituted nitroimidazoles measured by pulse-radiolysis, J. Chem. Soc., Faraday Trans. 76 (1976) 1377–1390.

[55] R.J. Knox, R.C. Knight, D.I. Edwards, Interaction of nitroimidazole with DNA in vitro—structure–activity-relationships, Br. J. Cancer 44 (1981) 741–745.

[56] G.X. Chen, P.P. Ong, L. Ting, DFT approach for electron affinity of negative atomic ions, Chem. Phys. Lett. 290 (1998) 211–215.

[57] C.A. Reynolds, W.G. Richards, Theoretical calculation of electrode-potentials—electron-withdrawing compounds, Int. J. Quant. Chem. 41 (1992) 293–310.

[58] C.A. Reynolds, Theoretical electrode-potentials and conformational energies of benzoquinones and naphthoquinones in aqueous-solution, J. Am. Chem. Soc. 112 (1990) 7545–7551.

[59] C.F. Fischer, J.B. Lagowski, S.H. Vosko, Ground states of CA- and SC- from two theoretical points-of-view, Phys. Rev. Lett. 59 (1987) 2263–2266.

[60] T. Wymore, X. Gao, T.C. Wong, Molecular dynamics simulation of a solvated dodecylphospocholine micelle, Biophys. J. 76 (1999) A57.

[61] J. Tomasi, B. Mennucci, E. Cances, The IEF version of the PCM solvation method: an overview of a new method addressed to study molecular solutes at the QM ab initio level, J. Mol. Struct., THEOCHEM 464 (1999) 211–226.

[62] R. Cammi, M. Cosssi, B. Mennucci, J. Tomasi, Theoretical Aspects of Biochemical Reactivity, Khuwer Academic Publishing, France, 1997.

[63] E. Cances, B. Mennucci, J. Tomasi, A new integral equation formalism for the polarizable continuum model: theoretical background and applications to isotropic and anisotropic dielectrics, J. Chem. Phys. 107 (1997) 3032–3041.

[64] G.E. Adams, E.D. Clarke, I.R. Flockhart, R.S. Jacob, D.S. Sehmi, I.J. Startfor, P. Wardman, M.E. Watts, Structure–activity relationships in the development of hypoxic cell radiosensitizers: I. Sensitization efficiency, Int. J. Radiat. Biol. 35 (1979) 133–150.

[65] G.E. Adams, E.D. Clarke, I.R. Flockhart, R.S. Jacob, D.S. Sehmi, I.J. Startfor, P. Wardman, M.E. Watts, Structure–activity relationships in the development of hypoxic cell radiosensitizers: II. Cytotoxicity and therapeutic ratio, Int. J. Radiat. Biol. 35 (1979) 151–160.

[66] J.R. Pires, C. Saito, S.L. Gomes, A.M. Giesbrecht, A.T. Amaral, Investigation of 5-nitrofuran derivatives: synthesis, antibacterial activity, and quantitative structure–activity relationships, J. Med. Chem. 44 (2001) 3673–3681.

[67] G. Chauviere, B. Bouteille, B. Enanga, C. Albuquerque, S.L. Croft, M. Dumas, J. Perie, Synthesis and biological activity of nitro heterocycles analogous to megazol, a trypanocidal lead, J. Med. Chem. 46 (2003) 427–440.

[68] K. Benakli, T. Terme, J. Maldonado, A convenient synthesis of highly conjugated 5-nitroimidazoles, Heterocycles 57 (2002) 1689–1695.

[69] P. Wardman, E.D. Clarke, R.S. Jacobs, A. Minchinton, M.R.L. Stratford, M.E. Watts, M. Woodcock, M. Moazzam, J. Parrick, R.G. Wallace, C.E. Smithen, in: L.W. Brady (Ed.), Radiation Sensitizers: Their Use in the Clinical Management of Cancer, Masson, New York, NY, 1980, pp. 83–90.

[70] E.D. Clarke, P. Wardman, Oxygen inhibition of nitroreductase-electron-transfer from nitro radical-anions to oxygen, Biochem. Biophys. Res. Commun. 69 (1976) 942–949.

[71] J.C. Rienstra-Kiracofe, G.S. Tschumper, H.F. Schaefer III, Atomic and molecular electron affinities: photoelectron experiments and theoretical computations, Chem. Rev. 102 (2002) 231–282.